Vol. 57: 51–60, 2013
doi: 10.3354/cr01147

CLIMATE RESEARCH
Clim Res

Published online June 27

A new methodology for weighting high-resolution model simulations to project future rainfall in the Middle East

Rana Samuels*, Maayan Harel, Pinhas Alpert

Department of Geophysics and Planetary Sciences, Faculty of Exact Sciences, Tel Aviv University, Tel Aviv 69978, Israel

ABSTRACT: A divergence metric was used to combine 4 high-resolution climate models to generate more reliable simulations of future rainfall. The approach is based on the assumption that the use of multiple models (an ensemble) is superior to the use of a single model, even if one of the models is shown to better capture past trends. Such an approach is especially useful in areas with steep climatic gradients, where large-scale climate models are not effective in capturing orographic and local effects. We applied the methodology to the Middle East, and specifically to Israel, where climate shifts from arid to humid temperate occur over a distance of around 400 km. Model weights were determined by calculating the similarity between the probability distributions of the models and those of the historical data using the Jenson-Shannon divergence metric. These weights were then applied to future model projections. Annual amounts of rainfall, numbers of wet days and numbers of 3 d wet spells were analyzed. Compared with observed data, the weighted ensemble outperformed the equal weights ensemble, which outperformed the best model. For the northern and central stations, average annual amounts of rainfall decreased in both near- and far-future periods, with most of the change occurring at the peak and in the left-hand tail and less change in the right-hand tail of the probability distribution. This, combined with the change in the right-hand tail of the distribution in numbers of wet spells in the near future, suggests that the decline in overall rainfall will be higher than the corresponding decline in extreme events; or in other words even though there will be less rainfall, the extreme events will remain, and even possibly increase. In the south, a mixed trend of slightly increasing median amounts of rainfall and slightly decreasing extreme events is projected.

KEY WORDS: RCM · Middle East rainfall · Weighted ensemble

1. INTRODUCTION

Understanding the implications of climate change on rainfall is critical for water management, agriculture and planning. In regions such as the Middle East, which has recently been shown to be a 'hot spot' of global climate change (Giorgi 2006), and where water resources are already scarce, such information can play a crucial role in optimizing development strategies. The best tools available for the prediction of future changes are climate models. Over the past few years, the use of ensembles, or combinations of multiple climate model results, has been suggested as a way of improving probabilistic simulations of future climate change (Collins 2007). These probabilistic scenarios can help better assess risk, and are useful in planning and devising mitigation strategies (Stott & Forest 2007, Lopez et al. 2009).

At both global and regional levels, it has been shown that different climate models vary in performance in different geographical regions; therefore, a combination of models will outperform a single model (Doblas-Reyes et al. 2000, Thomson et al. 2006, Weisheimer et al. 2009). However, there has been much debate as to whether unequal weighting outperforms equal weighting (e.g. Weigel et al. 2010,

*Email: ranas@post.tau.ac.il

DelSole et al. 2012). Due to uncertainty in the relationship between simulated present-day climate and simulated climate changes, a model simulation which exhibits a high amount of skill with regard to current or past climate does not necessarily provide a more accurate projection of climate change (Whetton et al. 2007, Räisänen et al. 2010, Räisänen & Ylhäisi 2011). Though we are aware of these limitations, in this study, we have used the best data available in an attempt to improve upon rainfall projections at the local level. Since much of the debate about weighting is due to the fact that different models are more skillful in different geographical regions, we hope that by focusing on a local level we can overcome this limitation. The Middle East in general and Israel in particular have been chosen, in part, because of the extremely sharp precipitation gradient in the region. This gradient causes considerable difficulties in reliable simulation, given the need for very high spatial resolution due to the importance of orographic effects, especially in the northern part of Israel (Giorgi & Lionello 2008). While the use of ensembles in this region is not a substitute for higher resolution data, the range of data provided by multiple simulations will hopefully enable more robust analysis. Under the assumption that weighting the models provides added value, it becomes necessary to assess what type of weighting would be most optimal. The challenge in creating such ensembles is how to best combine the varying simulations from different models. Recent attempts include allocating model weights according to inverse proportionality to the errors in forecast probability (Min et al. 2009), Bayesian optimal weighting schemes (Robertson et al. 2004), Bayesian hierarchical analysis (Sanso 2008) and pairwise dynamic combinations (Chowdhury & Sharma 2009).

For the Middle East, recent climate change studies have focused on results of individual regional climate model (RCM) configurations, including the MM5 (Smiatek et al. 2011) and the RegCM (Krichak et al. 2010, 2011, Samuels et al. 2011). On a local scale, the impacts of future climate change on the hydrology of the Jordan River (Samuels et al. 2010) and on water availability in the Sea of Galilee (Rimmer et al. 2011) have also been studied using single high-resolution climate model simulations. Within the limitations discussed above, we argue that ensembles can provide more skillful simulations here as well. In this paper, we present the use of a divergence metric to optimally weight different simulations and create ensemble probability distributions for chosen rainfall parameters at a local scale.

2. DATA SETS

2.1. Study area and historical data

The Middle East lies at the nexus of Asia, Europe and Africa and is characterized by steep precipitation gradients, high interannual rainfall variability (Alpert et al. 2008) and limited water resources (Gvirtsman 2002, Tal 2006). Here we focused on 13 stations located throughout Israel (Fig. 1; details of stations in Table 1). The average annual rainfall ranges from semi-arid (50 to 200 mm yr^{-1}) to temperate (200 to 600 mm yr^{-1}) to semi-humid (600 to 1200 mm yr^{-1}). Daily data from the stations for the years 1965–1999 were considered.

2.2. Climate models

Recently, simulations from rRCMs for the Middle East in general and Israel in particular have been generated as part of the GLOWA Jordan River project (www.glowa-jordan-river.de). This is a multinational, interdisciplinary project focusing on sustainable water management in the region. As water resources are directly linked to rainfall, climate sim-

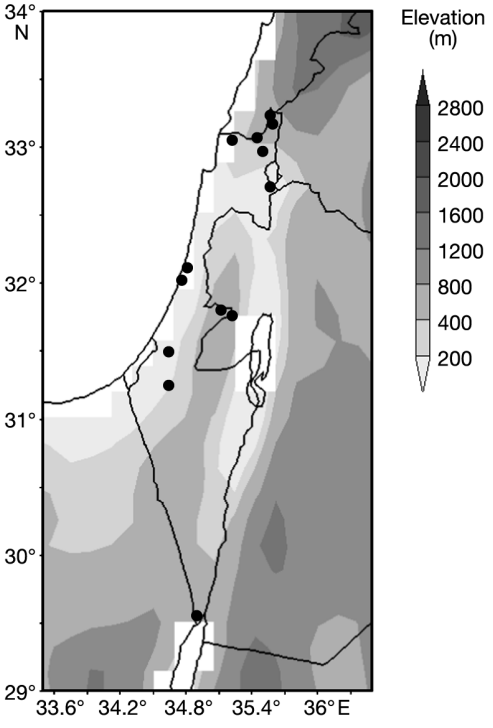

Fig. 1. Map showing locations of the 13 rainfall stations (dots). Topography is based on data from the climate-model version of the Japan Meteorological Agency's (JMA) operational numerical weather prediction model

Table 1. Locations of stations

Name	Latitude (N)	Longitude (E)
Kfar Giladi	33°14′	35°34′
Kfar Blum	33°10′	35°36′
Har Kenaan	32°59′	35°30′
Kibutz Kinerret	32°43′	35°34′
Yiron	33°04	35°27′
Eilon	33°03′	35°13′
Qiryat Shaul	32°07′	34°39′
Tel Aviv	32°01′	34°36′
Kiryat Anavim	31°48′	35°07′
Jerusalem	31°46′	35°13′
Dorot	31°30′	34°38′
Beer Sheva	31°15′	34°38′
Eilat	29°33′	34°39′

ulations are an important aspect of this project. Four climate simulations currently in use are generated by 2 versions of the MM5 regional model (MM5 3.5 and MM5 3.7) (Smiatek et al. 2010); 1 set is driven by the ECHAM5-MPI general circulation model (GCM) and the second is driven by the UK Met Office HadCM3 GCM. Another RCM simulation is the ICTP RegCM regional model driven by the ECHAM5-MPI GCM (Krichak et al. 2010, 2011). Given the similarity between the MM5 3.5 and MM5 3.7 versions, only the 2 simulations from the MM5 3.5 version were used here.

Another high-resolution global simulation is based on a climate-model version of the Japan Meteorological Agency's (JMA) operational numerical weather prediction model, with a horizontal grid size of about 20 km (Mizuta et al. 2006, Kitoh et al. 2008, Jin et al. 2009). Currently, this is the only GCM available at this resolution. While the 3 RCM models used in our study (ECHAM-MM5v3.5, Hadley-MM5v3.5 and ECHAM-RegCM) provide transient climate simulations from 1960 to 2060, the JMA experiment is a time slice experiment with a validation period (1979–2007) and a near-future simulation (2015–2035). All simulations assume the SRES (Special Report on Emissions Scenarios) greenhouse gas emissions scenario A1B which contains a balanced emphasis on all energy sources. For all models, precipitation data for the 13 chosen stations was calculated using inverse distance weighting (IDW) from the nearest gridpoints.

3. METHODOLOGY

3.1. General structure

To identify changes in both mean and extreme events over time, statistical distributions, such as cumulative probability and probability density functions (PDFs), are often used. Here we compared the PDFs for different time periods in order to identify future shifts in both mean and extreme amounts of rainfall. First we compared the observed data from 13 stations with model simulations for past/current climate. Then we compared the modeled simulations for the current era with simulations for the future, to obtain a sense of expected future change.

Fig. 2 shows the PDFs for Kfar Giladi from the observed data and 4 models. PDFs for annual amounts of rainfall (in mm), numbers of wet days and numbers of 3 d wet spells per season (October–April) are shown. The PDFs were calculated using a normal kernel function. A wet day was considered a day with rainfall >1 mm. The different models have different skill with regard to each chosen parameter. For the observed data and 3 of the models, the 29 yr period from 1970–1999 was used. For the JMA model, the 29 yr period from 1979–2007 was used.

There were 2 steps to the process: validation and projection. For validation, we combined the PDFs from the 4 models into a single PDF and then compared it with the PDF from the observed data. Once we had determined that the calculated PDF captured the spread of historical data, we applied the same methodology for future time periods in order to calculate the projected future PDF. Future PDFs were compared with the PDF of the historical period to identify future shifts and changes.

3.2. Jensen-Shannon divergence

The combination of models was done using the Jenson-Shannon (JS) divergence metric, a method of measuring the similarity between 2 distributions (Lin 1991). This metric is based on the widely used information-theory measure of divergence: Kullback-Leibler (KL). However, KL is not a metric (e.g. is not symmetric, does not satisfy triangle inequality) so it is inappropriate for measuring and comparing distances between numerous models. JS can be viewed as a modification of KL that makes it a metric. JS has been widely applied in computational sciences, including bioinformatics, genomic comparisons and protein surface comparisons (Ofran & Rost 2003, Sims et al. 2009, Itzkovitz et al. 2010). One of its features makes it particularly useful for the case of multi-model analysis: it can assign a different weight to each probability distribution. The metric is calculated as follows:

$$JS_{\pi}(p_1, p_2) = H(\pi_1 p_1 + \pi_2 p_2) - \pi_1 H(p_1) - \pi_2 H(p_2) \quad (1)$$

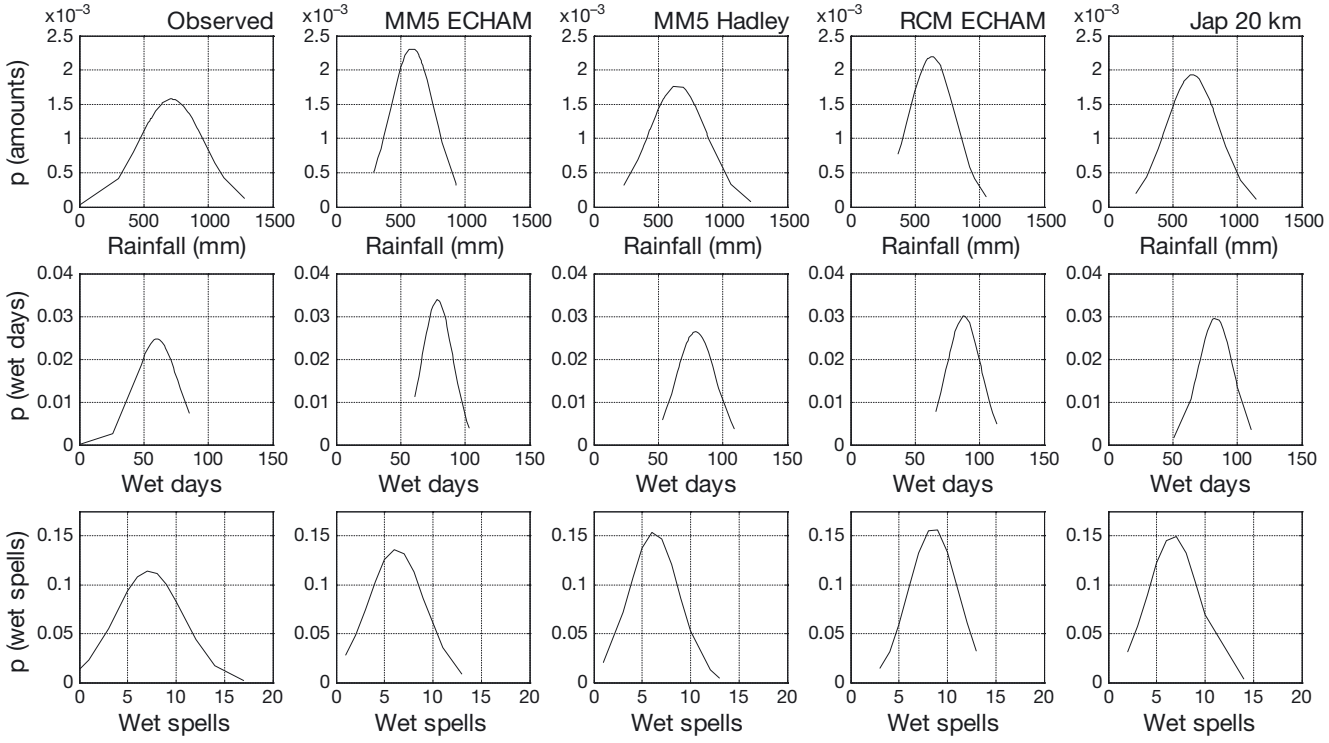

Fig. 2. Probability density functions (PDF) for Kfar Giladi for observed data and 4 models (see Section 2.2) of annual amounts of rainfall, numbers of wet days and numbers of 3 d wet spells per season are shown

where p_1 and p_2 are the probability distribution functions (each 0.5 in this case) and π_1 and π_2 are the weights of the probability distributions p_1 and p_2, respectively, with the constraints that $\pi_1, \pi_2 \geq 0, \pi_1 + \pi_2 = 1$. H is the Shannon entropy function, which is a measure of uncertainty and is calculated as follows:

$$H(\mathbf{x}) = -\sum_{i=1}^{n} p(x_1) \log_b p(x_1) \quad (2)$$

where $\mathbf{x}$ is a vector of variables and b is the base of the logarithm used. The most common base used is 2, which was also chosen for this study. It can be seen in Eq. (1) that the JS divergence is the entropy of the average minus the average of the entropies.

JS values range between 0 and 1, with 0 being the most similar and 1 being the most divergent. It should be noted that the JS score is a unitless value and its importance in our case lies in its relative value to the other JS scores.

The JS divergence was calculated for all models compared with the historical data for the past time period. Since lower JS divergence numbers are associated with models with higher similarity to the observed data, the inverse of these numbers was used to calculate the weights given to each of the models. The weight for each model was calculated as:

$$w_i = \frac{1/\mathrm{JSD}_i}{\sum_{i=1}^{N} \mathrm{JSD}_i} \quad (3)$$

where w_i is the weight for each model i, JSD_i is the calculated JS divergence between model i and the historical data and N is the number of models (here 4). It should be noted that $\sum_{i=1}^{N} w_i = 1$. Once the weights were determined, PDFs from the 4 models were combined to create a single ensemble PDF.

4. BOOTSTRAPPING

One of the problems in attempting to determine the weights of different models is that an independent validation dataset must be created. In order to meet this requirement, given that we had only 29 yr of past data, the bootstrapping method was employed. The process of calculating weights was done for a randomly selected sample of data. Out of the 29 yr dataset we randomly selected a sample of 20 yr from each model and from the observed data. The weights were calculated for this random sample, and a single ensemble PDF was created. The JS divergence metric was then calculated by comparing the weighted

Table 2. Calculated weights of the different climate models based on the Jenson-Shannon divergence values between each model and the observed dataset for rainfall amounts, the numbers of wet days and the numbers of 3 d wet spells. Calculated weights and ranks are given for each model. For model descriptions see Section 2.2

Location	ECHAM-MM5		Hadley-MM5		ECHAM-RegCM		JMA	
	Weight	Rank	Weight	Rank	Weight	Rank	Weight	Rank
Annual average amounts								
Kfar Giladi	0.24	4	0.24	1	0.28	3	0.23	2
Kfar Blum	0.25	2	0.20	3	0.35	1	0.20	4
Har Knaan	0.27	2	0.20	4	0.31	1	0.22	3
Kibbutz Kinneret	0.27	2	0.14	4	0.34	1	0.24	3
Yiron	0.26	2	0.21	4	0.31	1	0.22	3
Eilon	0.22	3	0.21	4	0.34	1	0.23	2
Qiryat Shaul	0.23	3	0.14	4	0.36	1	0.27	2
Tel Aviv	0.26	1	0.20	4	0.27	3	0.27	2
Qiryat Anavim	0.21	2	0.19	4	0.36	1	0.25	3
Jerusalem	0.22	2	0.19	4	0.32	3	0.27	1
Dorot	0.26	1	0.21	3	0.26	4	0.27	2
Beer Sheva	0.18	4	0.21	3	0.38	1	0.24	2
Eilat	0.32	2	0.36	1	0.17	3	0.15	4
Number of wet days								
Kfar Giladi	0.26	4	0.23	2	0.26	3	0.25	1
Kfar Blum	0.25	3	0.22	4	0.29	2	0.25	1
Har Knaan	0.28	2	0.18	4	0.27	3	0.27	1
Kibbutz Kinneret	0.27	2	0.28	1	0.22	4	0.22	3
Yiron	0.26	2	0.21	4	0.31	1	0.22	3
Eilon	0.27	3	0.20	4	0.29	1	0.24	2
Qiryat Shaul	0.26	1	0.29	2	0.22	4	0.24	3
Tel Aviv	0.26	1	0.25	3	0.21	4	0.28	2
Qiryat Anavim	0.21	3	0.20	4	0.30	1	0.29	2
Jerusalem	0.24	2	0.18	4	0.30	1	0.28	3
Dorot	0.25	2	0.23	3	0.22	4	0.30	1
Beer Sheva	0.26	2	0.19	4	0.23	3	0.31	1
Eilat	0.33	1	0.29	2	0.17	4	0.21	3
Number of 3 d wet spells								
Kfar Giladi	0.22	3	0.27	1	0.25	4	0.26	2
Kfar Blum	0.24	2	0.27	1	0.28	3	0.22	4
Har Knaan	0.18	4	0.20	3	0.34	1	0.28	2
Kibbutz Kinneret	0.13	4	0.22	3	0.45	1	0.20	2
Yiron	0.29	2	0.16	4	0.33	1	0.22	3
Eilon	0.29	1	0.18	4	0.27	3	0.26	2
Qiryat Shaul	0.14	4	0.27	2	0.30	3	0.29	1
Tel Aviv	0.19	4	0.29	1	0.27	3	0.25	2
Qiryat Anavim	0.13	4	0.17	3	0.47	1	0.23	2
Jerusalem	0.10	4	0.17	3	0.53	1	0.19	2
Dorot	0.13	4	0.30	2	0.24	3	0.32	1

PDF from the 20 chosen years with a PDF created by the remaining 9 yr. This process of random selection followed by weight calculation was repeated 3000 times. The final weights (Table 2) and final JS divergence values (Table 3) used were the means of the 3000 sets.

5. ENSEMBLE COMPARISON

Table 2 shows the values of the weights calculated using the JS divergence bootstrapping method for each model, station and parameter. Next to the weight is a number between 1 and 4, indicating the rank of the model compared to the other models. There was no one best model for either a specific parameter or a specific station, though the ECHAM-RegCM seemed to best capture the annual amounts of rainfall, while the JMA best represented the numbers of wet days per season, with the ECHAM-MM5 coming in at a close second. In the case of 3 d wet spells, the JMA slightly outperformed the ECHAM-RegCM and was the best predictor. Table 3 shows the calculated JS divergence between the observed data compared with the calculated weighted PDF, equal weights and that of the best individual model. The best model was defined for each parameter as that with the lowest sum of ranks (Table 2). Generally, the weighted ensemble clearly outperformed the ensemble of equal weights which, in turn, outperformed the best model for all parameters (Fig. 3). Fig. 3 shows the fitted PDF for annual amounts of average rainfall for Kfar Giladi, Tel Aviv and Beer Sheva. It should be noted that in the figure, the non-weighted ensemble is very close to the weighted one. The slight differences can be better seen in Table 3.

6. FUTURE SIMULATIONS

Fig. 4 shows the calculated weighted PDF comparison of the historical period (1965–1994) and the observed data (left hand column), a PDF for the near future (2015–2035) compared with the past model (middle column) and a PDF of the far future (2036–2060) compared with the past model (right hand column). The amount of rainfall and the wet day parameters for 4 stations representing northern (top row), central (middle 2 rows) and southern (bottom row) Israel are shown. For near-future calculations, all 4 models were used. For far-future calculations, the

Table 3. Jenson-Shannon (JS) divergence for calculated probability density functions. Results for proportionally weighted calculations (JS divergence), equally weighted calculations (EW) and best models (BM) are shown for 13 stations and 3 parameters. Calculated weights and ranks are given for each model. NA: not available

Location	JS divergence		EW		BM	
	Weight	Rank	Weight	Rank	Weight	Rank
Annual precipitation amounts						
Kfar Giladi	0.0003	2	0.0003	1	0.0007	3
Kfar Blum	0.0006	2	0.0006	3	0.0004	1
Har Knaan	0.0004	1	0.0005	2	0.0005	3
Kibbutz Kinneret	0.0004	1	0.0005	2	0.0008	3
Yiron	0.0003	2	0.0003	3	0.0002	1
Eilon	0.0004	2	0.0004	3	0.0002	1
Qiryat Shaul	0.0006	1	0.0007	3	0.0006	2
Tel Aviv	0.0008	2	0.0008	1	0.0014	3
Qiryat Anavim	0.0014	1	0.0016	3	0.0015	2
Jerusalem	0.0012	1	0.0013	2	0.0018	3
Dorot	0.0010	1	0.0010	2	0.0025	3
Beer Sheva	0.0003	1	0.0005	2	0.0006	3
Eilat	0.0057	1	0.0076	2	0.0131	3
Number of wet days						
Kfar Giladi	0.0007	3	0.0007	2	0.0004	1
Kfar Blum	0.0001	2	0.0001	1	0.0001	3
Har Knaan	0.0001	1	0.0001	2	0.0001	3
Kibbutz Kinneret	0.0001	1	0.0002	2	0.0003	3
Yiron	0.0002	1	0.0002	2	0.0003	3
Eilon	0.0001	1	0.0001	2	0.0002	3
Qiryat Shaul	0.0002	1	0.0002	2	0.0004	3
Tel Aviv	0.0003	1	0.0003	3	0.0003	2
Qiryat Anavim	0.0001	1	0.0001	2	0.0002	3
Jerusalem	0.0002	1	0.0002	2	0.0004	3
Dorot	0.0004	2	0.0004	3	0.0003	1
Beer Sheva	0.0006	2	0.0007	3	0.0005	1
Eilat	0.0064	1	0.0071	2	0.0080	3
Number of 3 d wet spells						
Kfar Giladi	0.0014	1	0.0014	2	0.0022	3
Kfar Blum	0.0013	1	0.0013	2	0.0023	3
Har Knaan	0.0016	1	0.0018	3	0.0017	2
Kibbutz Kinneret	0.0045	1	0.0072	2	0.0080	3
Yiron	0.0014	1	0.0016	2	0.0025	3
Eilon	0.0010	1	0.0011	2	0.0022	3
Qiryat Shaul	0.0007	1	0.0008	2	0.0012	3
Tel Aviv	0.0020	2	0.0020	1	0.0025	3
Qiryat Anavim	0.0020	1	0.0043	2	0.0056	3
Jerusalem	0.0023	1	0.0049	2	0.0072	3
Dorot	0.0020	3	0.0018	2	0.0018	1
Beer Sheva	NA		NA		NA	
Eilat	NA		NA		NA	

JMA model was not used, as there were no simulations for the years 2035–2060. In this case, the weights were calculated for the 3 RCM models, again based on JS divergence values.

With regard to both annual amounts of rainfall and numbers of wet days, for the 3 more northernly stations, there was a clear shift to the left in both the near-future and far-future periods. As can be seen in Table 4, a more intense reduction occurred in the lower and middle percentiles (10 and 50) than in the higher percentiles (90 and 95). This suggests that, while the average amount of rainfall will decrease, extended rainfall events will still occur. The projections for Kfar Giladi were the most dramatic, with a far-future reduction of almost 25% in median precipitation amounts and a reduction of almost 15% in the number of wet days. For the central stations of Jerusalem and Tel Aviv the projections were less dramatic, but still suggest a reduction of between 5 and 15% in both rainfall amount and number of wet days in the lower and middle percentiles. The southern station of Beer Sheva exhibited a slightly different trend, with median rainfall days and amounts increasing slightly in both the near and far future. However, here the extremes of annual rainfall and number of wet days showed mixed results, with different signs of change for the near and far future. Since this is a region with average annual rainfall amounts of around 200 mm and number of rainfall days per year of around 35, even a change of 10% is not that great. Table 4 shows the expected rainfall changes based on equal weighting. Equal weighting seems to temper the changes to a certain extent in both far-future rainfall amounts and wet days. The changes in near-future rainfall amounts and wet days remained fairly similar, except for Beer Sheba, where, as we mentioned, large changes in percentages translate into small actual changes due to the low levels of rainfall occurring there.

7. DISCUSSION AND CONCLUSIONS

In spite of the limitations posed by the weak connection between current and future climate and the biases with respect to uncertainty in model simulations, the use of ensembles is now accepted practice in research involving global climate models; the same holds true for higher resolution models at regional and even local scales. Here we demonstrated the use of the JS divergence metric for generating such ensembles on a local level. The main advantage of using such a divergence metric is that it provides an objective way of quantifying the distance between different distributions in a consis-

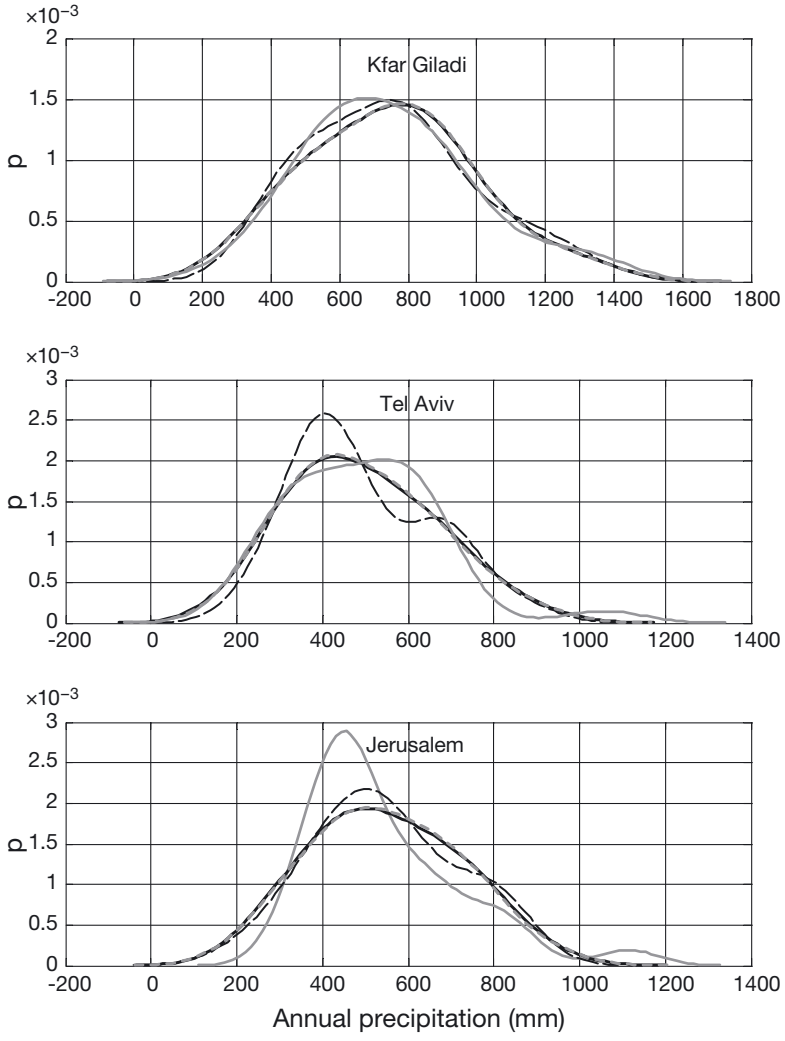

Fig. 3. Fitted probability density functions (PDF) for annual amounts of average rainfall for Kfar Giladi, Tel Aviv and Beer Sheva. Curves from observed data (continuous gray lines), as well as the proportionally weighted (Jenson-Shannon divergence; continuous black lines) and equally weighted (short dashed gray lines) ensembles and the best models (long dashed black lines) are shown

tent manner so that many models can be compared to the observed values as well as to each other. Assigning different weights to the models based on this calculation allows optimization of the predictive strengths of the different models. These strengths may lie in their simulation of specific parameters or in their level of accuracy for certain geographic locations. This is especially useful as we have shown that no one definitive best model exists for either the stations or the different parameters. It should be noted, however, that the metric cannot compensate for biases common to all of the models.

In addition, focusing on the PDFs of different rainfall parameters and the changes in their future distributions provides an accepted and relatively simple way of assessing change. The shifts in PDFs supply probabilistic information about mean and extreme values, both important components of water planning and management. Future predictions from our ensemble simulations support previous work, which shows a decrease of >20% in mean regional precipitation by 2060 (Shindell 2007, Smiatek et al. 2010, Krichak et al. 2011), with an increase in extreme events in both observed historical data (Alpert et al. 2002, 2008) and in future climate simulations by 2060 (Samuels et al. 2011). They also support historical studies showing a stronger decrease in the north than in the south in 1960–1990 compared to 1930–1960 (Ben-Gai et al. 1998). To further assess the benefit of unequal versus equal weighting, cross-validation of the simulated climate changes, as suggested by Räisänen et al. (2010), could be applied. This will be attempted in future research once more high-resolution simulations have become available.

Acknowledgements. We thank Gerhard Smiatek for preparing daily time series from the MM5 experiments and Shimon Krichak and Yoseph Breitgard for preparing data from the RegCM. This research was partly supported by a grant from the Israeli Water Authority. We thank Dr. Amir Givati for his assistance. We also thank 3 anonymous reviewers whose comments greatly helped to improve the manuscript.

Fig. 4. Change in Jenson-Shannon divergence calculated probability density function (PDF) over time (past, near future and far future) for (a) annual amounts of rainfall, (b) no. of wet days per season and (c) no. of 3 d wet spells per season. Left column shows observed data (gray) and calculated past (as in Fig. 3 above). Middle column shows near future (2015–2035; dashed lines) and calculated past (1965–1994; solid lines). Right-hand column shows far future (2035–2060; dashed lines) and calculated past (1965–1994; solid lines)

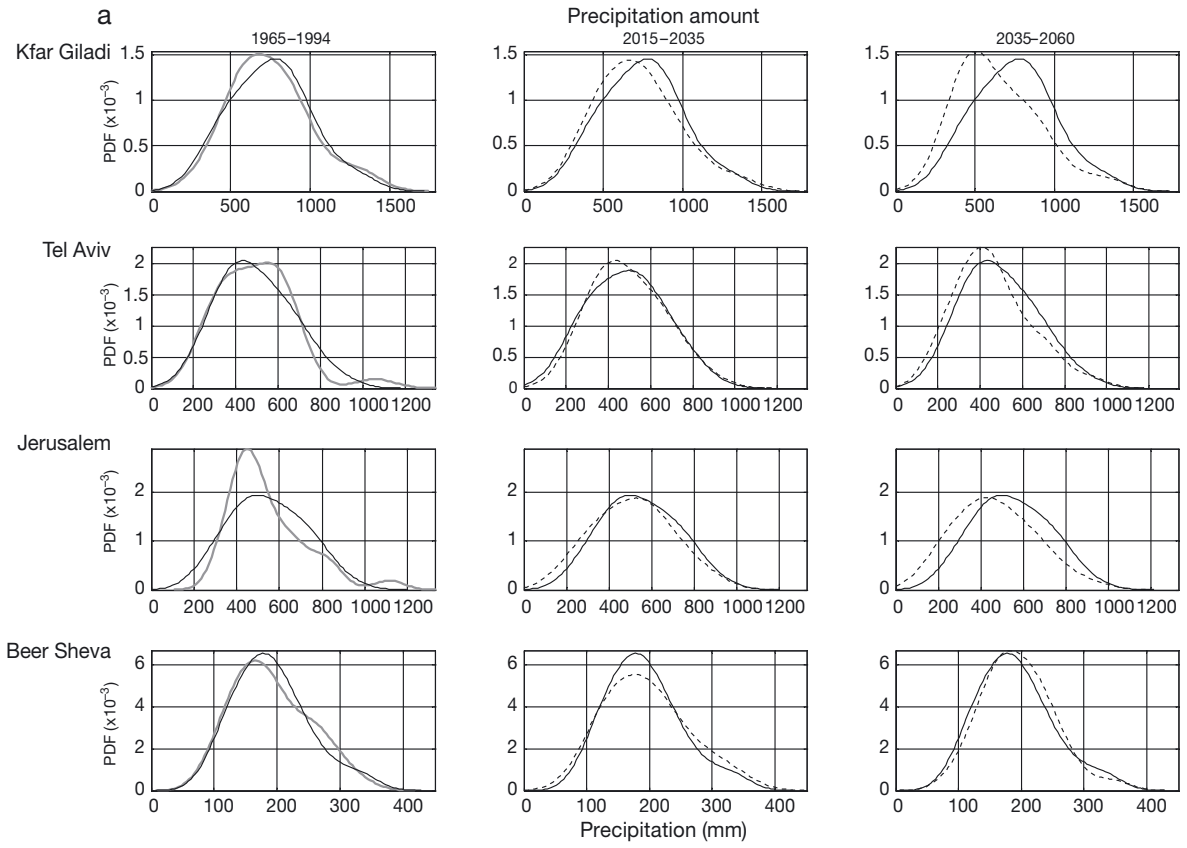
a
Precipitation amount
1965–1994
2015–2035
2035–2060
Kfar Giladi
Tel Aviv
Jerusalem
Beer Sheva
PDF (x10^{-3})
Precipitation (mm)

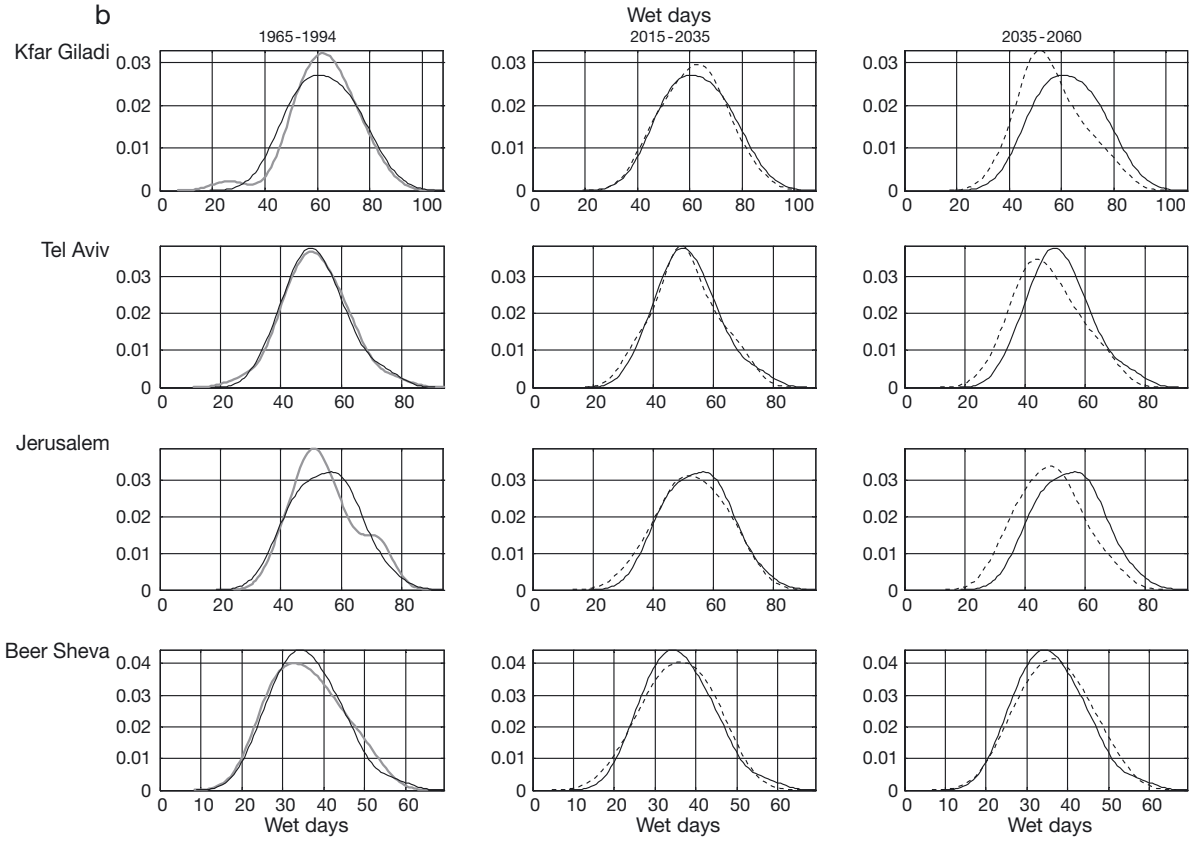
b
Wet days
1965-1994
2015-2035
2035-2060
Kfar Giladi
Tel Aviv
Jerusalem
Beer Sheva
Wet days

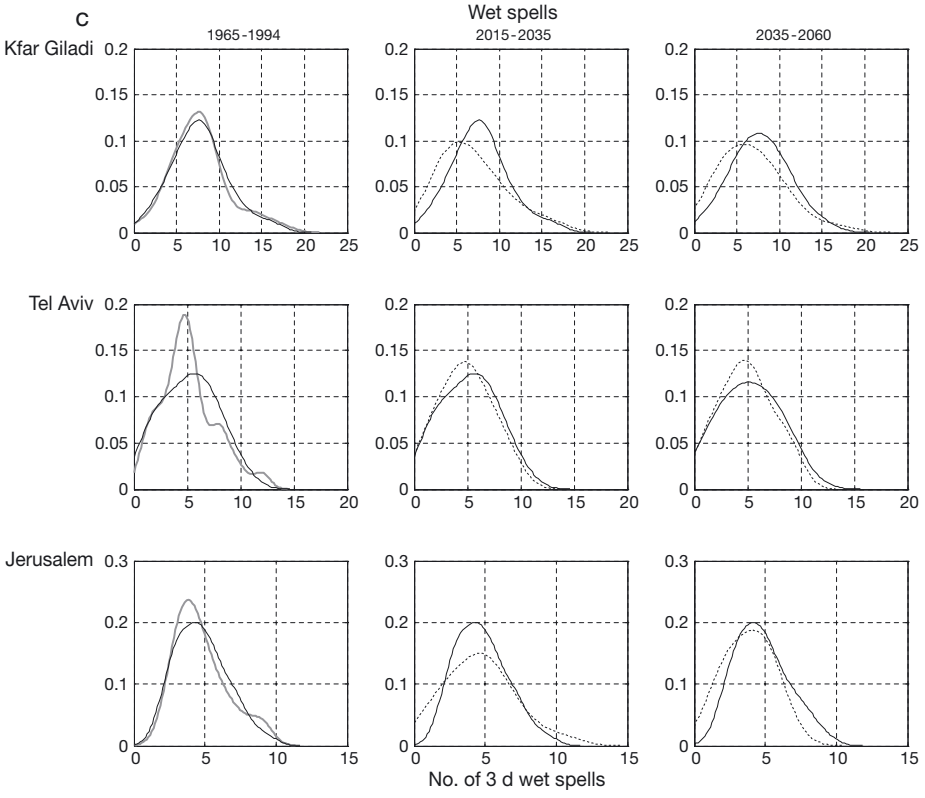

Table 4. Change in 10th, 50th, 90th and 95th percentile annual amounts of rainfall and numbers of wet days for the near future (2015–2035; NF) and far future (2035–2060; FF) for Jenson-Shannon (JS) divergence weighting and equal weighting. **Bold**: values with statistical significance above $\alpha = 0.05$

Location	Time period	Amounts of rainfall (%) 0.10	0.50	0.90	0.95	No. of wet days (%) 0.10	0.50	0.90	0.95
JS divergence weighting									
Kfar Giladi	NF	**–2.7**	**–8.0**	**–0.7**	**0.8**	**–3.8**	**–1.2**	**–1.2**	**–0.7**
	FF	**–14.9**	**–24.6**	**–8.0**	**–3.2**	**–10.3**	**–14.4**	**–4.7**	**–3.8**
Tel Aviv	NF	–11.5	–5.7	–0.7	–0.4	**–6.5**	**–1.4**	**2.0**	**–2.1**
	FF	–21.0	–9.8	–1.5	–1.7	**–8.0**	**–6.9**	**–2.3**	**–5.4**
Jerusalem	NF	**–17.2**	**–1.9**	**–3.4**	**2.1**	–7.7	–4.5	–2.0	–2.2
	FF	**–27.1**	**–16.4**	**–9.8**	**–2.2**	–15.6	–10.8	–7.2	–5.0
Beer Sheva	NF	2.1	2.8	8.7	2.2	**–1.9**	**1.2**	**–3.0**	**–1.4**
	FF	7.8	0.5	–1.8	–10.0	**3.3**	**3.9**	**3.0**	**3.6**
Equal weighting									
Kfar Giladi	NF	**–2.8**	**–8.5**	**–0.5**	**1.1**	**–3.8**	**–1.4**	**–1.1**	**–0.6**
	FF	**–13.3**	**–23.3**	**–5.9**	**–1.1**	**–8.8**	**–13.4**	**–4.2**	**–3.6**
Tel Aviv	NF	–11.0	–5.2	0.0	0.0	–6.0	–1.2	2.4	–1.6
	FF	–16.8	–7.0	0.6	0.2	–4.3	–2.5	2.5	–0.5
Jerusalem	NF	**–16.7**	**–2.4**	**–3.3**	**1.4**	–9.0	–5.4	–1.9	–1.4
	FF	**–28.2**	**–16.2**	**–8.8**	**1.3**	–12.6	–8.8	–4.1	–2.5
Beer Sheva	NF	0.7	1.9	6.7	1.1	–1.0	2.7	–2.0	–0.6
	FF	2.9	–3.2	–7.3	–14.7	–4.7	–1.6	–0.4	0.1

LITERATURE CITED

Alpert P, Ben-Gai T, Baharad A, Benjamini Y and others (2002) The paradoxical increase of Mediterranean extreme daily rainfall in spite of decrease in total values. Geophys Res Lett 29:31-1–31-4, doi:10.1029/2001GL013554

Alpert P, Krichak SO, Shafir H, Haim D, Osetinsky I (2008) Climatic trends to extremes: employing regional modeling and statistical interpretation over the E. Mediterranean. Global Planet Change 63:163–170

Ben-Gai T, Bitan A, Manes A, Alpert P, Rubin S (1998) Spatial and temporal changes in annual rainfall frequency distribution patterns in Israel. Theor Appl Climatol 61: 177–190

Chowdhury S, Sharma A (2009) Long range NINO3.4 predictions using pair wise dynamic combinations of multiple models. J Clim 22:793–805

Collins M (2007) Ensembles and probabilities: a new era in the prediction of climate change. Philos Transact A Math Phys Eng Sci 365:1957–1970

DelSole T, Yang X, Tippett M (2013) Is unequal weighting significantly better than equal weighting for multi-model forecasting? Q J R Meteorol Soc 139:176–183

Doblas-Reyes FJ, Deque M, Piedelievre JP (2000) Multi-model spread and probabilistic seasonal forecasts in PROVOST. Q J R Meteorol Soc 126:2069–2088

Giorgi F (2006) Climate change hot-spots. Geophys Res Lett 33:L08707, doi:10.1029/2006GL025734

Giorgi F, Lionello P (2008) Climate change projections for the Mediterranean region. Global Planet Change 63:90–104

Gvirtsman C (2002) Water resources of Israel. Yad Ben Tsvi, Jerusalem

Itzkovitz S, Hodis E, Segal E (2010) Overlapping codes within protein-coding sequences. Genome Res 20: 1582–1589

Jin F, Kitoh A, Alpert P (2009) Water cycle changes over the Mediterranean: a comparison study of a super-high-resolution global model with CMIP3. Philos Transact A Math Phys Eng Sci 368:1–13

Kitoh A, Yatagai A, Alpert P (2008) First super-high-resolution model projection that the ancient Fertile Crescent will disappear in this century. Hydrolog Res Lett 2:1–4

Krichak SO, Alpert P, Kunin P (2010) Numerical simulation of seasonal distribution of precipitation over the eastern Mediterranean with a RCM. Clim Dyn 34:47–59

Krichak S, Breitgand J, Samuels R, Alpert P (2011) A double-resolution transient RCM climate change simulation experiment for near-coastal eastern zone of the eastern Mediterranean region. Theor Appl Climatol 103:167–195

Lin J (1991) Divergence measures based on the Shannon entropy. IEEE Trans Inf Theory 37:145–151

Lopez A, Fung F, New M, Watts G, Weston A, Wilby RL (2009) From climate model ensembles to climate change impacts and adaptation: a case study of water resource management in the southwest of England. Water Resour Res 45:W08419, doi:10.1029/2008WR007499

Min YM, Kryjov VN, Park CK (2009) A probabilistic multi-model ensemble approach to seasonal prediction. Weather Forecast 24:812–828

Mizuta R, Oouchi K, Yoshimura H and others (2006) 20-km-mesh global climate simulations using JMA-GSM model—mean climate states. J Meteorol Soc Jpn 84:165–185

Ofran Y, Rost B (2003) Analysing six types of protein–protein interfaces. J Mol Biol 325:377–387

Räisänen J, Ylhäisi JS (2011) Can model weighting improve probabilistic projections of climate change? Clim Dyn 39:1981–1998

Räisänen J, Ruokolainen L, Ylhäisi J (2010) Weighting of model results for improving best estimates of climate change. Clim Dyn 35:407–422

Rimmer A, Givati A, Samuels R, Alpert P (2011) Using ensemble of climate models to evaluate future water and solutes budgets in Lake Kinneret, Israel. J Hydrol (Amst) 410:248–259

Robertson AW, Lall U, Zebiak SE, Goddard L (2004) Improved combination of multiple atmospheric GCM ensembles for seasonal prediction. Mon Weather Rev 132:2732–2744

Samuels R, Rimmer A, Hartmann A, Krichak S, Alpert P (2010) Climate change impacts on Jordan River flow: downscaling application from a regional climate model. J Hydrometeorol 11:860–879

Samuels R, Smiatek G, Krichak S, Kunstmann H, Alpert P (2011) Extreme value indicators in highly resolved climate change simulations for the Jordan River area. J Geophys Res 116:D2412, doi:10.1029/2011JD016322

Sanso TCB (2008) Joint projections of temperature and precipitation change from multiple climate models: a hierarchical Bayesian approach. J R Stat Soc A 172:83–106

Shindell D (2007) Estimating the potential for twenty-first century sudden climate change. Philos Transact A Math Phys Eng Sci 365:2675–2694

Sims GE, Jun SR, Wu G, Kim SH (2009) Alignment-free genome comparison with feature frequency profiles (FFP) and optimal resolutions. Proc Natl Acad Sci USA 106:2677–2682

Smiatek G, Kunstmann H, Heckl A (2010) High resolution climate change simulations for eastern Mediterranean and Jordan River region. Geophys Res Abstr 12:EGU 2010–EGU11251

Smiatek G, Kunstmann H, Heckl A (2011) High resolution climate change simulations for the Jordan River Area. J Geophys Res 116:D16111, doi:10.1029/2010JD015313

Stott PA, Forest CE (2007) Ensemble climate predictions using climate models and observational constraints. Philos Transact A Math Phys Eng Sci 365:2029–2052

Tal A (2006) Seeking sustainability: Israel's evolving water management strategy. Science 313:1081–1084

Thomson MC, Doblas-Reyes FJ, Mason SJ, Hagedorn R and others (2006) Malaria early warnings based on seasonal climate forecasts from multi-model ensembles. Nature 439:576–579

Weigel AP, Knutti R, Liniger MA, Appenzeller C (2010) Risks of model weighting in multimodel climate projections. J Clim 23:4175–4191

Weisheimer A, Doblas-Reyes FJ, Palmer TN, Alessandri A and others (2009) ENSEMBLES: a new multi-model ensemble for seasonal-to-annual predictions: skill and progress beyond DEMETER in forecasting tropical Pacific SSTs. Geophys Res Lett 36:L21711, doi:10.1029/2009GL040896

Whetton P, Macadam I, Bathols J, O'Grady J (2007) Assessment of the use of current climate patterns to evaluate regional enhanced greenhouse response patterns of climate models. Geophys Res Lett 34:L14701, doi:10.1029/2007GL030025

Editorial responsibility: Filippo Giorgi, Trieste, Italy

Submitted: July 2, 2012; Accepted: December 19, 2012
Proofs received from author(s): June 12, 2013